

# 10 kHz repetitive high-resolution TV Thomson scattering on TEXTOR

H. J. van der Meiden,<sup>a)</sup> C. J. Barth, T. Oyevaar, S. K. Varshney, and A. J. H. Donné  
*FOM-Institute for Plasma Physics Rijnhuizen, Association EURATOM-FOM, P.O. Box 1207, 3430 BE  
 Nieuwegein, The Netherlands*

M. Yu. Kantor and D. V. Kouprienko  
*Ioffe Institute, RAS, Saint Petersburg, 194021, Russia*

A. Alexeev  
*MultiTech Ltd., Saint Petersburg, 198103, Russia*

W. Biel and A. Pospieszczyk  
*Institut für Plasmaphysik, Forschungszentrum Jülich, D-52425 Jülich, Germany*

(Presented on 20 April 2004; published 7 October 2004)

In December 2003 a new 10 kHz multiposition Thomson scattering diagnostic with high spatial resolution has become operational on the TEXTOR tokamak. The system is the follow up of the high-resolution double-pulse Thomson scattering diagnostic. The conventional ruby laser has been replaced by a 10 kHz intracavity laser system and the spectrometer detector has been upgraded with two ultrafast complementary metal–oxide–semiconductor cameras combined with a special image intensifier stage. In the initial phase of operation, a burst of 18 pulses decaying from 17 to 8 J, with a repetition rate of 5 kHz, could be extracted from the laser. At a laser energy up to 12 J per pulse, ten electron temperature and density profiles were measured with an observational error of 10% on the electron temperature ( $T_e$ ) and 5% on the electron density ( $n_e$ ) at  $n_e = 2.5 \times 10^{19} \text{ m}^{-3}$  per spatial element of 12 mm. The resolution of the detection optics enables to sample either the full plasma diameter of 900 mm with 120 spatial channels of 7.5 mm each, or a 160 mm long edge chord with 98 spatial channels of 1.7 mm each. © 2004 American Institute of Physics.  
 [DOI: 10.1063/1.1786646]

## I. INTRODUCTION

In 2000 and 2001, double-pulse TV Thomson scattering (TS) was performed on the TEXTOR tokamak ( $R_0 = 1.75 \text{ m}$ ,  $a = 0.46 \text{ m}$ ,  $B_0 < 2.8 \text{ T}$ , and  $I_p < 0.8 \text{ MA}$ ). This TS system was based on a double-pulse ruby laser ( $2 \times 12 \text{ J}$ ) and two intensified charge coupled device cameras for recording the scattered light. The resemblance of the detector to a TV camera has led to the name TV Thomson scattering. It was capable to measure two electron temperature ( $T_e$ ) and density ( $n_e$ ) profiles during one discharge along a vertical chord of 900 mm length (at  $R = 1840$ ) with 120 spatial channels of 7.5 mm each.<sup>1,2</sup> The double-pulse TS system is not suited to study the dynamics of mesoscale structures like magnetohydrodynamic islands and internal transport barriers in hot plasmas. To explore these phenomena, one needs a time resolution of  $< 1 \text{ ms}$ . Therefore, a repetitive TS system is developed, consisting of a repetitive laser and a fast detection system. The Ioffe Institute in St. Petersburg and MultiTech Ltd. designed and constructed a so-called double-pass intracavity laser.<sup>3,4</sup> The system is operating like a normal laser oscillator, however in this case the plasma is part of an 18 m long cavity. To preserve the high spatial resolution of the diagnostic as well as to adapt as much as possible to the existing viewing optics, the beam path of the new laser is kept the same as that of the double-pulse laser.

<sup>a)</sup>Electronic mail: meiden@rijnh.nl

A state of the art detector has been constructed, based on two 12-bit Phantom V7.0 complementary metal–oxide–semiconductor (CMOS) cameras and a special image intensifier stage. A comprehensive description of the full system will be given by Barth *et al.*<sup>5</sup> In this article, a brief description of the TS system will be presented along with some first results.

## II. INTRACAVITY LASER

In Fig. 1 the basic elements of the laser are shown. The laser cavity is formed by a flat rear mirror and spherical end mirror ( $f = 4.5 \text{ m}$ ). In this way the laser beam passes twice through the tokamak plasma along the same path before returning into the laser rod ( $19 \times 200 \text{ mm}^2$ , 0.05% Cr<sup>+</sup>). The cavity is designed such, that it provides a high pumping to probing energy conversion.

The  $Q$  state of the cavity is switched by a Pockels' cell. The laser system is in principle capable to produce, during a flash lamp period of 10 ms, a burst of 40 pulses of 10–15 J each, with a repetition rate of 10 kHz. For comparison, a conventional  $Q$ -switched three-stage ruby laser provides only 1.6 J<sup>6</sup> and 0.8 J per pulse<sup>7</sup> at a repetition rate of 10 and 250 kHz, respectively. Balancing the pumping and probing energy during 5–10 ms sets extremely high demands on the flash lamp load and the power supply accuracy. For this very reason, MultiTech Ltd. constructed a 380 kJ power supply,

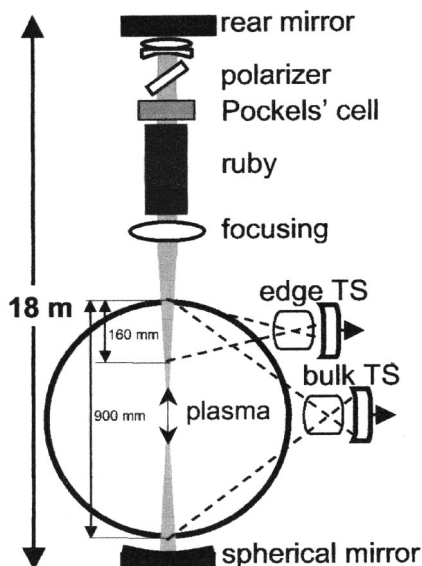


FIG. 1. Schematic view of intracavity laser, the TEXTOR vessel is part of it. Both viewing systems for edge and full chord TS are also shown.

which is capable to deliver pure rectangular flash lamp pumping pulses of more than 5 MW during 10 ms.

In Fig. 2(a), a burst of 18 laser pulses is shown, corresponding to a total probing energy of 236 J. Combining this with the flash lamp load of 15 kJ a conversion efficiency of 1.6% is found. The pulse widths vary between 1.0 and 2.0  $\mu\text{s}$  full width at half maximum [Fig. 2(b)]. The full-angle divergence of the laser is smaller than 0.7 mrad, containing 90% of the energy, resulting in a beam waist of 3 mm in the plasma. It can be seen, that during the burst the pulse energy drops to half of the initial value. This behavior is not yet fully understood. However, measurements show that the amplification process occurs dominantly at the periphery of the

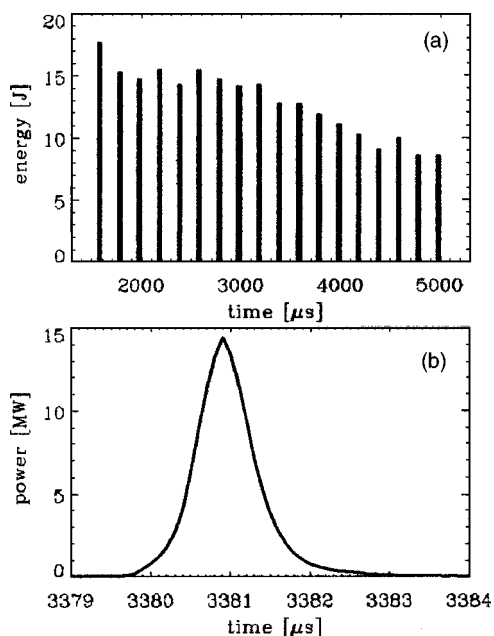


FIG. 2. (a) Burst of 18 laser pulses, showing that even operating with a ruby with a high dope (0.05%  $\text{Cr}^+$ ) enables the generation of high pulse energies. (b) The pulse shape of one of the pulses.

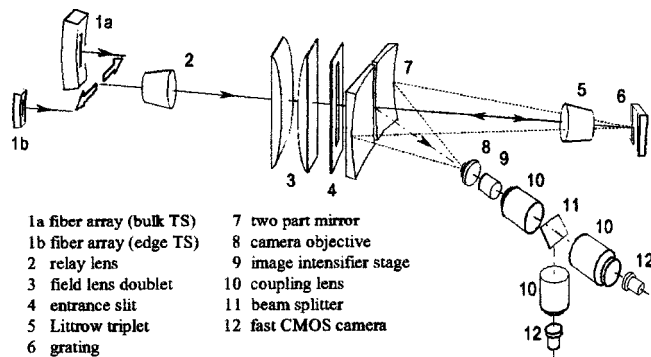


FIG. 3. Spectrometer layout of the multipulse TS system.

ruby rod cross section. It is obvious, that due to this local pumping, thermal-lensing effects cannot be neglected. In the summer of 2004 a rod with a 0.03%  $\text{Cr}^+$  will be installed, enabling laser amplification more homogeneously over the cross section of the rod. Preliminary test measurements with a low dope rod confirmed that a significant improvement of pumping to probing conversion efficiency and divergence is possible.

### III. DETECTION SYSTEM

In Fig. 3 the basic elements of the detection branch are shown: relay optics, polychromator, and detector.

Scattered light is collected, at  $f/20.5$  for bulk TS and  $f/10.3$  for edge TS, by multielement lenses and transmitted via two different fiber arrays over a distance of 28 m to a Littrow polychromator. One fiber array is sampling the full plasma diameter of 900 mm and the other is sampling the edge chord of 160 mm. A seven-element lens system (item 2) images the fiber output onto the entrance slit (item 4) of the spectrometer. To suppress vessel stray light, the grating is oriented such that light at the laser wavelength returns along its original path. The spectrum is projected onto a two-part spherical mirror (item 7), which serves for pupil imaging.

The spectrometer covers a spectral range of 585–800 nm. Using a motor controlled rotation table different gratings can be selected covering different temperature ranges: a 600 lp/mm for  $100 \text{ eV} \leq T_e \leq 5 \text{ keV}$ , a 900 lp/mm grating for  $50 \text{ eV} \leq T_e \leq 2 \text{ keV}$  and a 1500 lp/mm grating for  $5 \text{ eV} \leq T_e \leq 500 \text{ eV}$  especially for edge TS.

Finally, the spectral image at the mirror of  $260 \times 200 \text{ mm}^2$  is imaged onto the cathode of the detector (image size  $23.4 \times 18 \text{ mm}$ ) by a camera objective. The image intensifier stage consists of a Gen III image intensifier ( $\eta = 50\%$  @ 585–800 nm) equipped with a P46 screen in combination with a stack of three proximity-focused intensifiers. This setup enables the Gen III microchannel plate to operate without electron depletion during a train of  $> 50$  laser pulses. This is the result of the rather low gain ( $G_{\text{ph}} = 150$ ) of the Gen III, which is piled up by the intensifier stack to a total gain of  $10^5$ . A tandem lens system (items 10) combined with a 50% beamsplitter (item 11) images the P46 output screen of the image intensifier stage onto the chip of two CMOS cameras. Phantom V7.0 cameras have been applied because of the following specs: image format  $512 \times 384$  pixels at

10 900 frames/s, pixel size  $22 \mu\text{m}$ , inverted sensitivity 50 photons/cnt and effective dynamic range 10 bit. It was found that the cameras suffer from residual signal image-to-image crosstalk. Illuminating the chip with diffused bias light could reduce this effect to  $<2\%$ .

With the described detection system the electron temperature (50 eV–5 keV) and density profiles along a full chord (120 spatial channels of 7.5 mm) can—in principle—be measured with an observational error of 8% on  $T_e$  and 4% on  $n_e$  at  $n_e = 2.5 \times 10^{19} \text{ m}^{-3}$  using a laser energy of 15 J.

#### IV. PERFORMANCE AND RESULTS

To capture the TS photons during the full laser pulse the image intensifier needs to be gated during  $2 \mu\text{s}$ . This discloses one of the main critical points of this diagnostic: the competition between plasma background light and the TS signal. Therefore, the background is measured additional to every laser pulse to be able to correct for this. In the first campaign, the  $Q$  state of the cavity was not optimized; i.e., old deteriorated vacuum windows introduced losses in the cavity. Although the relative plasma light contribution was about the same as the TS signal,  $T_e$  and  $n_e$  profiles could be measured with a spatial resolution of 12 mm, and with a relative error of 10% and 5%, respectively.

In Fig. 4 a sequence of ten  $T_e$  and  $n_e$  profiles is shown, with a time separation of  $200 \mu\text{s}$ . The last eight observed profiles are not shown, because the corresponding laser energy dropped to values lower than 8 J. Island-like structures are visible, however, there was no opportunity to probe the islands around a time instant where the islands  $O$  points were crossing the laser chord.

The sum of two relativistic spectral distribution functions, reflecting the spectral shapes corresponding to back and forward Thomson scattering, is fitted to the experimental data to find the width and area of the spectra to obtain  $T_e$  and  $n_e$ , respectively.

With a look to the future, the power supply of the laser was prepared to provide four bursts of pulses with a time

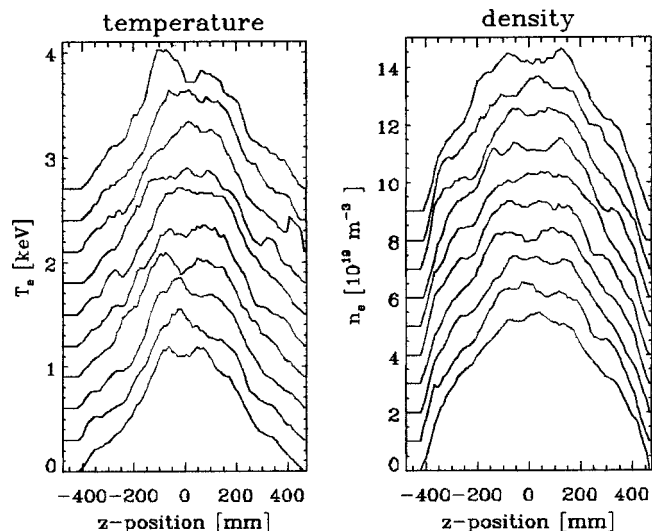


FIG. 4. First ten of 18  $T_e$  and  $n_e$  profiles, recorded every  $200 \mu\text{s}$ , smoothed over four spatial points. The corresponding laser energy ranged from 1.2 to 8 J. The profiles for  $T_e$  and  $n_e$  are plotted above each other with an equidistance of 0.3 keV and  $1 \times 10^{19} \text{ m}^{-3}$ , respectively.

separation of  $>1$  s. In the summer of 2004, this operation mode will be investigated. The goal is to produce 40 pulses of about 15 J, at a repetition rate of 10 kHz, during each of the four bursts.

#### ACKNOWLEDGMENTS

This work, supported by the European Communities under the contract of Association between EURATOM/FOM, was carried out within the framework of the European Fusion Programme with financial support from NWO.

<sup>1</sup>C. J. Barth *et al.*, Rev. Sci. Instrum. **72**, 1138 (2001).

<sup>2</sup>C. J. Barth *et al.*, Rev. Sci. Instrum. **70**, 763 (1999).

<sup>3</sup>M. Yu. Kantor *et al.*, Rev. Sci. Instrum. **72**, 1159 (2001).

<sup>4</sup>M. Yu. Kantor and D. V. Kouprienko, Rev. Sci. Instrum. **70**, 780 (1999).

<sup>5</sup>C. J. Barth *et al.*, Rev. Sci. Instrum. (to be published).

<sup>6</sup>R. Behn *et al.*, Appl. Opt. **36**, 363 (1980).

<sup>7</sup>J. M. Grace *et al.*, Opt. Eng. **37**, 2205 (1998).